ELSEVIER

Available online at www.sciencedirect.com

SCIENCE DIRECT®

International Journal of Solids and Structures 43 (2006) 2050–2063

INTERNATIONAL JOURNAL OF SOLIDS and STRUCTURES

www.elsevier.com/locate/ijsolstr

A direct finite element method study of generalized thermoelastic problems

Xiaogeng Tian *, Yapeng Shen, Changqing Chen, Tianhu He

The State Key Laboratory of Mechanical Structural Strength and Vibration, The School of Civil Engineering and Mechanics, Xi'an Jiaotong University, Xianning West Road 28, Xi'an 710049, PR China

Received 9 December 2004; received in revised form 13 June 2005
Available online 22 August 2005

Abstract

By using the principle of virtual work, the finite element equations corresponding to the generalized thermoelasticity with two relaxation times (i.e., the G–L theory) are derived. In order to improve the accuracy of integral transform method, especially in two/three-dimension, the equations are solved directly in time-domain. As numerical examples, the developed method is used to investigate the generalized thermoelastic behavior of a slim strip and a semi-infinite plate subject to thermal shock loading. The results demonstrate that the developed method can faithfully predict the deformation of the structure and most importantly the delicate second sound effect of heat conduction in both one and two-dimensional solids whilst it is usually difficult to model, especially in two-dimensional, by using the transform method. This method can also be used to study generalized piezothermoelastic and magnetothermoelastic problems.

Keywords: Heat conduction; Generalized thermoelasticity; Finite element method; Second sound effect; Thermal shock

1. Introduction

Non-isothermal problems of elastic theory are the key problems of many engineering applications and have become increasingly important during the second half of last century, e.g., the intense thermal stresses due to the aerodynamic heating of high speed aircrafts, the extremely high temperatures and temperature

* Corresponding author. Tel.: +86 29 82668751; fax: +86 29 82669093.
E-mail address: tiansu@mail.xjtu.edu.cn (X. Tian).

0020-7683/$ - see front matter
doi:10.1016/j.ijsolstr.2005.06.071

gradients originating inside nuclear reactor; and especially the rapid change of heating in recently developed *ultra-fast* pulsed lasers in which the heat pulse operates in an order of pico-second or less (applications of *ultra-fast* laser ranges from micromachining (Zhu et al., 1999), non-destructive detection (Bonello et al., 1999), materials characterization (Hostetler et al., 1998), among others).

A common feature of the aforementioned problems is that the in-service environments are extremes: temperature and temperature gradient are high whilst the operation time period is as short as pico-second, giving rise to thermal shock. In those extreme cases, some characteristics (e.g., the heat wave propagation phenomena) cannot be successfully captured by the classical theory of thermoelasticity which implies that heat conduction occurs at an infinite speed. As a result, we have to resort to the generalized theories of thermoelasticity. The first theory of this type was developed by Lord and Shulman (1967) (usually referred to as the L–S theory). They considered isotropic solids and introduced one relaxation time parameter into the Fourier heat conduction equation, i.e., both the heat flux and its time derivative are considered in the heat conduction equation. The heat equation associated with this theory is thus hyperbolic. A direct consequence is that the paradox of infinite speed of propagation inherent in both the uncoupled and coupled theories of classical thermoelasticity is eliminated and the heat wave feature can be modeled by the generalized thermoelasticity. The L–S theory was later extended by Dhaliwal and Sherief (1980) to the case of anisotropic media. Uniqueness of solution for the generalized thermoelasticity under a variety of conditions was proved by Ignaczak (1979) and Sherief and Dhaliwal (1980), respectively. A feasible state space approach to problems of the generalized thermoelasticity was introduced by Anwar and Sherief (1988).

Generalized theories of thermoelasticity with two relaxation time parameters have also been proposed. Based on a generalized inequality of thermodynamics, Green and Lindsay (1972) developed the theory of thermoelasticity with two relaxation time parameters (named as the G–L theory). The G–L theory doesn't violate the Fourier's law of heat conduction when the body under consideration has a center of symmetry. In this theory, both the equations of motion and heat conduction are hyperbolic but the equation of motion is modified and differs from that of classical coupled thermoelasticity theory. Using the G–L theory, Erbay and Suhubi (1986) investigated the longitudinal wave propagation. A one-dimensional thermo-mechanical shock problem was studied by Sherief (1994) using a state space method developed earlier for the G–L theory (Sherief, 1993).

These two generalized thermoelasticity theories have been successfully applied to explore the thermal shock problems. In one-dimensional problems, the Laplace transform and inverse Laplace transform method can be used to provide the solutions. The calculated temperature distribution is found to exhibit a feature similar to that of the Heaviside function $H(t - a_0 x)$ (He et al., 2003), where t is time, a_0 is a constant and x is the distance from the heat source to the considered position, which implies that the heat wave front traverses at a *finite speed* of $1/a_0$ and that the temperature field within the region $x > t/a_0$ is not disturbed by the heat source. In two-dimensional problems, both Laplace and Fourier transforms and their inverse counterparts have to be used simultaneously (Sherief and Megahed, 1999). Usually, their inverse transforms can only be obtained numerically due to the complication of the corresponding expressions. However, the obtained result (Sherief and Megahed, 1999; Chen and Weng, 1989), in contrast to analytical inverse transform, shows no clear jump in the temperature field. Identification of the heat wave front and prediction of the second sound effect (as it should be) are thus not obvious. One of possible reasons may lie in the insufficiently accurate of the numerical inverse Laplace and Fourier transforms. Even in one-dimensional problem, if the inverse Laplace transformation obtained by numerical method, the jump in the temperature is not as obvious as obtained theoretically (Ei-caramany and Ezzat, 2004). In fact, there always exist numerical stability problems in calculating the inverse transforms by noting that the time period in thermal shock problems is as short as pico-second. Therefore, the applicability of the Laplace and Fourier transform method to two/three-dimensional generalized thermoelastic problems is limited.

An alternative choice to solve two/three-dimensional problems in the generalized thermoelasticity is through the finite element method. Chen and Weng proposed a generalized finite element model for the

coupled transient behavior of generalized thermoelastic solids. The time dependence was evaluated in the Laplace transform domain. They have used the developed finite element method to study the generalized thermoelastic response of a square cylinder with elliptical hole (Chen and Weng, 1988) and an axisymmetric circular cylinder (Chen and Weng, 1989). The same as introduced above, the jump of the temperature in the heat wave front is not obvious in the numerical solutions. The solutions can't present the wave properties of the heat conduction in very short time clearly (Chen and Weng, 1989).

In this paper, the finite element equations for two-dimensional generalized thermoelastic problems are derived within the framework of the G–L theory, with the obtained finite element equations solved directly in time domain. The proposed methodology is then applied to investigate the heat conduction of a slim strip (an approximate to one-dimensional problem) and a half space (a two-dimensional problem) subject to a heat source. For both one and two-dimensional problems, the obtained results demonstrate clearly that there exists a jump in the temperature field and the jump moves at a finite speed. Moreover, the displacements and the stress owing to the thermal disturbance are also investigated.

2. Finite element equations

In this section, the governing equations of generalized thermoelasticity (the G–L theory) are summarized, followed by the corresponding finite element equations. The G–L theory of generalized thermoelasticity consists of the equilibrium equation

$$\sigma_{ij,j} + \rho f_i = \rho \ddot{u}_i \tag{1}$$

the heat transfer equation

$$\rho T \dot{\eta} = -q_{i,i} + \rho h \tag{2}$$

and the Fourier's heat conduction law

$$q_i = -k_{ij}\theta_{,j} \tag{3}$$

where σ_{ij} is the stress, f_i is the body force, ρ is the mass density, u_i is the displacement, η is the entropy density, q_i is the heat flux, h is the heat source density, k_{ij} is the thermal conductivity coefficient, and $T = T_0 + \theta$ is the absolute temperature with θ and T_0 denoting the temperature changed and the reference temperature, respectively. In Eqs. (1)–(3), super-dot refers to the derivative with respect to time; comma followed by sub-index denotes the corresponding partial differentiation, and summation convention over repeated sub-indices applies.

Since only linear behavior is considered in this paper, the following linear constitutive equations are adopted, i.e.,

$$\begin{aligned} \sigma_{ij} &= C_{ijkl}\varepsilon_{kl} - \beta_{ij}(\theta + \tau_1 \dot{\theta}) \\ \rho\eta &= \beta_{ij}\varepsilon_{ij} + c_E\left(\theta + \tau_2 \dot{\theta}\right) \end{aligned} \tag{4}$$

where C_{ijkl} is the elastic stiffness, $\varepsilon_{ij} = (u_{i,j} + u_{j,i})/2$ is the strain, β_{ij} is the thermal constant, and c_E is the specific heat capacity. It is noted that the G–L theory differs from the classical theory of thermoelasticity in that two relaxation time parameters τ_1 and τ_2 are involved in the constitutive equations (4). When τ_1 and τ_2 vanish identically, the G–L theory reduces to the classical thermoelasticity.

It should be noted that appropriate boundary conditions associated with the governing Eqs. (1)–(3) must be adopted in order to properly formulate a problem. When the displacement and temperature are prescribed on the surfaces A_u and A_θ, respectively, one has

$$u_i = \bar{u}_i \quad \text{on } A_u \quad \text{and} \quad \theta = \bar{\theta} \text{ on } A_\theta \tag{5}$$

where $\bar{u}_i$ and $\bar{\theta}$ are the prescribed values. On the other hand, if surface traction and surface flux are applied to the corresponding surfaces A_σ and A_q, the following boundary conditions must be satisfied,

$$T_i = \sigma_{ji} n_j = \overline{T}_i \quad \text{on } A_\sigma \quad \text{and} \quad Q = q_i n_i = \overline{Q} \quad \text{on } A_q \tag{6}$$

where $\overline{T}_i$ and $\overline{Q}$ are the given surface traction and flux, respectively.

The finite element equations of a generalized thermoelasticity problem can be readily obtained by following the standard procedure (see, for example, (Prevost and Tao, 1983)). In the finite element method, the displacement component $\{u\}$ and temperature θ are related to the corresponding nodal values $\{u^{(e)}\}$ and $\{\theta^{(e)}\}$ by

$$\{u\} = [N]_{p\times n}\{u^{(e)}\} \quad \theta = [N']_{1\times n}\{\theta^{(e)}\} \tag{7}$$

where $p = 2$ for the two-dimensional problems considered here, n is the number of nodes per element, and $[N]$ and $[N']$ are the shape functions for the displacement and temperature, respectively. With Eq. (7), the strain $\{\varepsilon\}$ and temperature gradient $\theta'_i = \theta_{,i}$ can be expressed in terms of the nodal quantities $\{u^{(e)}\}$ and $\{\theta^{(e)}\}$ as

$$\{\varepsilon\} = [B]\{u^{(e)}\} \quad \theta' = [B']\{\theta^{(e)}\} \tag{8}$$

The principle of virtual work for the generalized thermoelasticity is

$$\int_V \left\lfloor \delta\{\varepsilon\}^{\mathrm{T}}\{\sigma\} + \delta\theta' q - \delta\theta\rho T_0\dot{\eta} \right\rfloor \mathrm{d}V = \int_V \delta\{u\}^{\mathrm{T}}(\rho\{f\} - \rho\{\ddot{u}\})\,\mathrm{d}V + \int_{A_\sigma} \delta\{u\}^{\mathrm{T}}\{\overline{T}\}\,\mathrm{d}A + \int_{A_q} \delta\theta\overline{Q}\,\mathrm{d}A \tag{9}$$

Substituting the constitutive relations (4) and Eq. (8) and neglecting the body force (the body force is not considered here), the finite element equations corresponding to Eqs. (1)–(3), (5) and (6) can be obtained as

$$\sum_{e=1}^{\mathrm{ne}} \left(\begin{bmatrix} M_{11}^{(e)} & 0 \\ 0 & M_{22}^{(e)} \end{bmatrix} \begin{Bmatrix} \ddot{u}^{(e)} \\ \ddot{\theta}^{(e)} \end{Bmatrix} + \begin{bmatrix} 0 & -C_{12}^{(e)} \\ C_{21}^{(e)} & C_{22}^{(e)} \end{bmatrix} \begin{Bmatrix} \dot{u}^{(e)} \\ \dot{\theta}^{(e)} \end{Bmatrix} + \begin{bmatrix} K_{11}^{(e)} & -K_{12}^{(e)} \\ 0 & K_{22}^{(e)} \end{bmatrix} \begin{Bmatrix} u^{(e)} \\ \theta^{(e)} \end{Bmatrix} = \begin{Bmatrix} F_1^{(e)} \\ -F_2^{(e)} \end{Bmatrix} \right) \tag{10}$$

where ne is the total number of elements. The coefficients in Eq. (10) and the right hand force vectors $\{F_1^{(e)}\}$ and $\{F_2^{(e)}\}$ are given below.

$$\begin{aligned}
&\left[M_{11}^{(e)}\right] = \int_{V^{(e)}} \rho[N]^{\mathrm{T}}[N]\,\mathrm{d}V \qquad \left[M_{22}^{(e)}\right] = \tau_2 \int_{V^{(e)}} c_E\rho[N']^{\mathrm{T}}[N']\,\mathrm{d}V \\
&\left[C_{12}^{(e)}\right] = \tau_1 \int_{V^{(e)}} [B]^{\mathrm{T}}[\beta][N']\,\mathrm{d}V \qquad \left[C_{21}^{(e)}\right] = T_0 \int_{V^{(e)}} [N']^{\mathrm{T}}[\beta][B']\,\mathrm{d}V \\
&\left[C_{22}^{(e)}\right] = \int_{V^{(e)}} c_E T_0[N']^{\mathrm{T}}[N']\,\mathrm{d}V \qquad \left[K_{11}^{(e)}\right] = \int_{V^{(e)}} [B]^{\mathrm{T}}[C][B]\,\mathrm{d}V \\
&\left[K_{12}^{(e)}\right] = \int_{V^{(e)}} [B]^{\mathrm{T}}[\beta][N']\,\mathrm{d}V \qquad \left[K_{22}^{(e)}\right] = \int_{V^{(e)}} [B']^{\mathrm{T}}[k][B']\,\mathrm{d}V \\
&\left\{F_1^{(e)}\right\} = \int_{A_\sigma} [N]^{\mathrm{T}}\{\overline{T}\}\,\mathrm{d}A \qquad \left\{F_2^{(e)}\right\} = \int_{A_\theta} [N']^{\mathrm{T}}\overline{Q}\,\mathrm{d}A
\end{aligned} \tag{11}$$

For numerical convenience, the following non-dimensional quantities are introduced

$$\begin{aligned}
&x^* = c_1\xi x, \quad y^* = c_1\xi y, \quad u_i^* = c_1\xi u_i, \quad t^* = c_1^2\xi t, \quad \tau_i^* = c_1^2\xi\tau_i \\
&\sigma_{ij}^* = \frac{\sigma_{ij}}{\mu}, \quad \theta^* = \frac{\theta}{T_0}, \quad \xi = \frac{\rho c_E}{\kappa}, \quad c_1^2 = \frac{\lambda + 2\mu}{\rho}, \quad i = 1, 2
\end{aligned} \tag{12}$$

where λ and μ are the Lame constants. Note that c_1 is the propagating velocity of elastic wave in the solid. As a result, the dimensionless elastic wave velocity is 1. With the dimensionless variables defined by Eq. (12), the finite element equation (10) is transformed into and solved in the non-dimensional space. Without causing ambiguity, the asterisk symbol of the non-dimensional variables is dropped off in the following for the sake of brevity.

3. Generalized heat conduction

The finite element equation (10) can be solved by the transform technology as in (Chen and Weng, 1988, 1989). In one-dimensional problem, Eq. (10) is transformed into Laplace domain and solved, then the results are transformed back to time domain via the inverse Laplace transform. In two-dimensional problems, Fourier transform should be used besides Laplace transform. The equations are solved in transformed domain and then results are transformed back into time domain via inverse Laplace and Fourier transform. If the considered structure is complicated or in the finite element analysis, the inverse transform (Laplace and Fourier transform) must be done in numerical form. However, numerical evaluation of inverse transform of Eq. (10) is very time consuming and is difficult to produce high resolution results for thermal shock problems. In three-dimensional problem, another integral transform should be added and the solving procedure will be more complicated and time consuming. As a result, some delicate features expected in generalized thermoelastic problems (e.g., the second sound effect of the heat conduction (He et al., 2003)) cannot be faithfully captured by the transform technology (Ei-caramany and Ezzat, 2004; Sherief and Helmy, 2002). According to the property of wave equation, the velocity of heat conduction specified by Eq. (10) in Sherief and Helmy (2002) is $1/\sqrt{\tau_0}$. The non-dimensional relaxation time τ_0 is 0.02, so the non-dimensional speed of the wave is 7.07 and the heat wave front should at about $x = 0.35$ at time $t = 0.05$. That means the temperature vanishes identically when $x > 0.35$. But the temperature approaches 0 until when $x > 0.69$ and it decrease to zero gradually in Sherief and Helmy (2002). That means the heat conducting at a finite speed has not been captured exactly.

In addition to the transform method, Eq. (10) can also be solved directly using an implicit–explicit algorithm as described in Prevost and Tao (1983). In the implicit–explicit algorithm, the stiffness and damping matrices have to be divided into implicit and explicit, which renders it difficult to implement the method into engineering analysis. Boundary element method was also used to solve the dynamic poroelastic and thermoelastic problem without integral transform (Chen and Dargush, 1995).

In this paper, the governing equation (10) is solved directly in time domain. The precision losing of transform method and the difficulties in implicit–explicit algorithm will be avoided. Because of the large gradient of temperature in the heat wave front, the grid size near the heat wave front need be very small. So the structure should be remeshed during the analysis due to the heat wave propagation in the structure. We will proceed to show that the method proposed here is capable of producing reliable results. To this end, two numerical examples are investigated using the developed method.

4. Numerical examples

4.1. A slim strip problem

The first example is a half infinite long slim strip as shown in Fig. 1. The boundary of the strip is traction free and subjected to a thermal loading $\theta = H(t)$ at one end AB and $q = 0$ along other boundaries BC, CD and DA, where $H(t)$ is the Heaviside function. The reference temperature is $T_0 = 293$ °C. The edge CD is constrained. In the analysis model, the dimension in the x-direction is much greater than that in the y-direc-

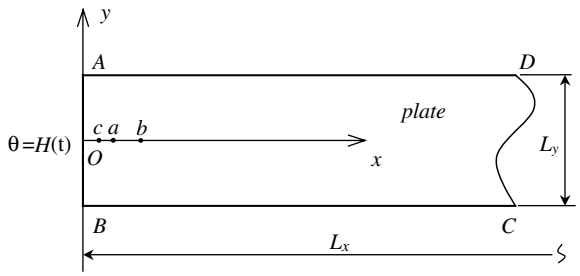

Fig. 1. A slim strip with thermal shock at the end AB.

tion ($L_x \gg L_y$) and neither elastic wave nor heat is reflected from the end CD during the analysis. In the simulation, $L_x = 1$, $L_y = 0.02$. This problem is chosen to mimic the generalized thermoelastic one-dimensional problem examined in He et al. (2003). Note that the thermal conduction along the slim strip is one-dimensional in essence. The slim strip is assumed to be made of isotropic material, with the mass density $\rho = 8945\text{kg/m}^3$, Posson's ratio $v = 0.3$, the Lame's constants $\lambda = 77.6$ GPa and $\mu = 38.6$ GPa, thermal expand coefficient is 1.78e−5 m/°C m, and the relaxation time parameters $\tau_1 = \tau_2 = 0.05$. Mesh sensitivity study has been conducted to ensure the convergence of the numerical results.

The finite element method predicted temperature distributions along the x-axis are shown in Fig. 2 for the instants $t = 0.080$ and 0.120. The feature can be clearly identified from the curves shown in Fig. 2, i.e., sharp jumps of the temperature exist around $x = 0.36$ and 0.54 for $t = 0.080$ and 0.120, respectively. It is further noted that on the right hand side of the jumps the temperature is essentially undisturbed (ignore the slight oscillation due to numerical noise), indicating that the temperature jumps correspond the heat wave front and that in the generalized thermoelasticity the heat conducts at a finite speed instead of an infinite velocity as implied in the classical theory of thermoelasticity. We can also find in Fig. 2 that the magnitude of the temperature jump reducing with the time passes. That means the jump will be vanished after a long time. This is accordant with the temperature distribution when time is long (the classical heat conduction) qualitatively.

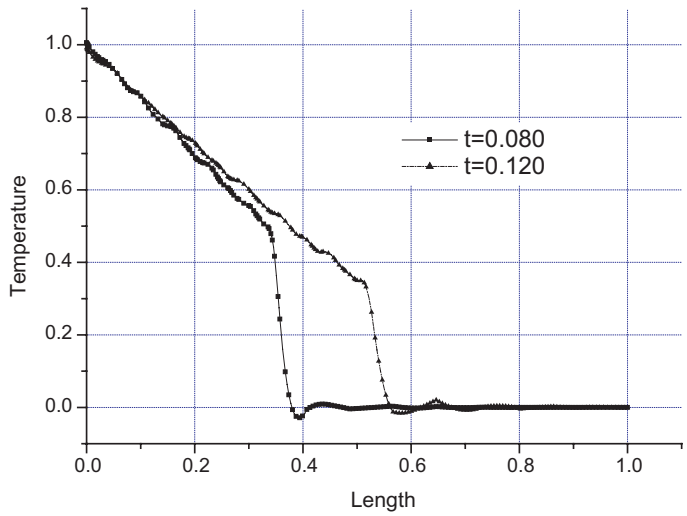

Fig. 2. The temperature of the plate along x-axis.

In fact, the positions of the temperature jumps in Fig. 2 can be inferred as follows by noting that it corresponds to the heat wave front. In the generalized thermoelasticity the thermal conduction equation can be expressed in the non-dimensional form as (Sherief and Megahed, 1999),

$$\nabla^2\theta = \frac{\partial\theta}{\partial t} + \tau_2\frac{\partial^2\theta}{\partial t^2} + \frac{\gamma}{k\xi}\frac{\partial}{\partial t}\left(\frac{\partial u_x}{\partial x} + \frac{\partial u_y}{\partial y}\right) \tag{13}$$

where $\gamma = (3\lambda + 2\mu)\alpha_t$, α_t is thermal expand coefficient. According to the property of wave equation, the dimensionless velocity of heat conduction specified by Eq. (13) is $v_h = 1/\sqrt{\tau_2}$. Obviously, the velocity of heat conduction will be infinite when $\tau_2 = 0$, consistent with that of the classical heat conduction theory. Recall that the dimensionless velocity of elastic wave is 1, the velocity of the heat conduction is thus $1/\sqrt{\tau_2}$ times of the elastic wave. Since the relaxation time parameter in the simulation is $\tau_2 = 0.05$, so the heat conduction velocity is $v_h = 4.472$. The heat wave fronts at $t = 0.08$ and 0.12 are at

$$x_1 = \frac{1}{\sqrt{0.05}} \times 0.08 = 0.358 \tag{14}$$

$$x_2 = \frac{1}{\sqrt{0.05}} \times 0.12 = 0.537 \tag{15}$$

We can see that results given by Fig. 2 are in good agreement with above predictions (Eqs. (14) and (15)), implying that the finite element results are reliable.

Time histories of the temperature for two spatial points '*a*' and '*b*' indicated in Fig. 1 are plotted in Fig. 3. The coordinate of '*a*' and '*b*' are (0.1, 0) and (0.3, 0), respectively. Abrupt temperature change is observed at different time for points '*a*' and '*b*'. According to the positions of '*a*' and '*b*' and the velocity of the heat wave front, the abrupt change should occur at time $0.022(0.1/v_h)$ and $0.067(0.3/v_h)$. These are almost the same with the positions of the abrupt changes in Fig. 3.

Fig. 4 shows the variations of the displacement component u_x along the x-axis at time $t = 0.08$ and 0.12. Since the right end of the slim strip is constrained, the left end of the strip moves to the left (negative displacement) when it is exposed to heating. It is shown in Fig. 4 that the displacement varies from negative to

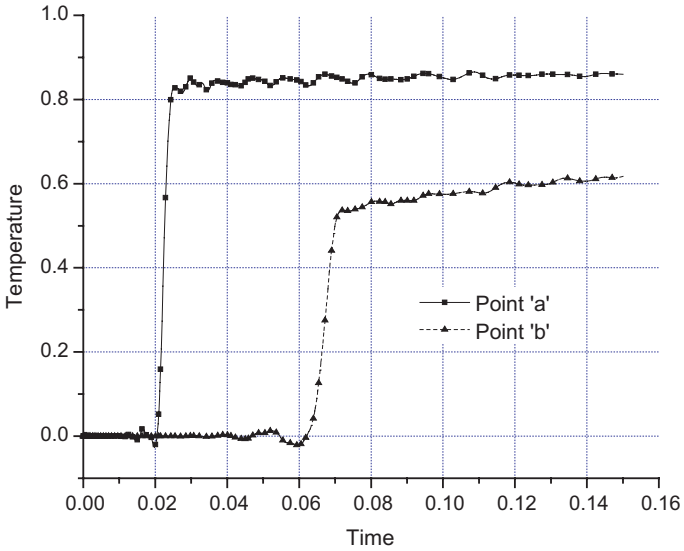

Fig. 3. Time history of the temperatures at different locations.

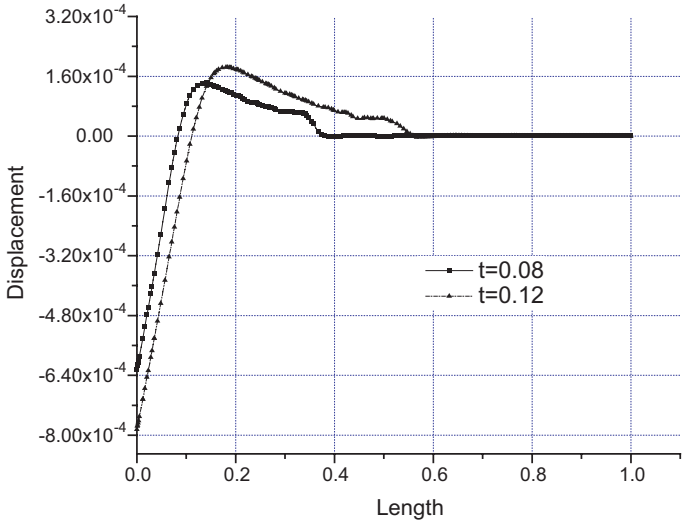

Fig. 4. The displacement distribution along the axis-x at different time.

positive and reduces to zero beyond the heat wave front continuously. The positive displacement behind the heat wave front is believed relates to the elastic wave propagation, the speed of which is smaller than that of the heat wave.

Time history of the x component displacements at different location is shown in Fig. 5. Point 'c' is on the x-axis and its x-coordinate is 0.05. From Fig. 5 we can see that the origin (O) moves to the left as soon as it is subject to the heat source. The speed is large at the beginning and gradually slows down until almost a constant value is reached. Point 'c' stays undisturbed for a while, corresponding to the duration of the heat conducting from origin to point 'c'($t = 0.05/v_h = 0.011$). This is consistent with the idea that heat conducts

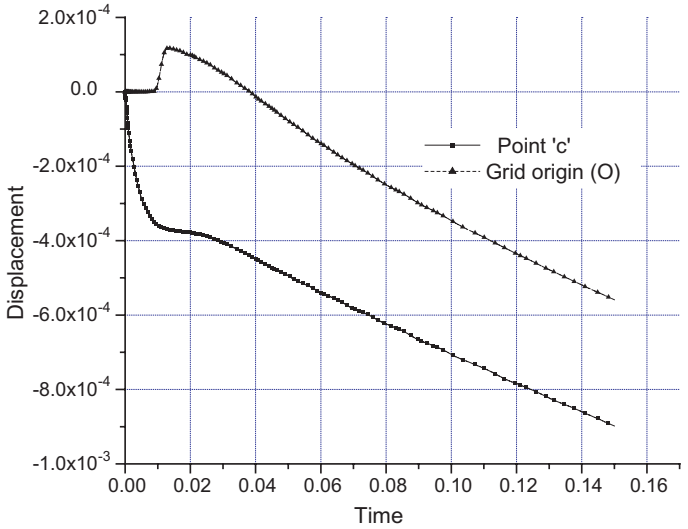

Fig. 5. The displacement of different location.

at a finite velocity in generalized thermoelasticity. When the heat wave front reaches at point '*c*', it moves to the right at first and then moves to the left after the elastic wave arrives.

4.2. A half space problem

In order to show whether the developed method is able to reveal the expected delicate features (e.g., the second sound effect of heat) in two-dimensional problems in generalized thermoelasticity, the second example is a half space subject to a heat source. The material properties are assumed to be the same as that of the slim strip. As shown in Fig. 6a, the boundary of the half space is traction free and subjected to a heat source of intensity $R(y,t) = H(a - |y|)H(t)$ along $x = 0$, where a is a constant. Due to the symmetry of the problem, only a quarter of the space (i.e., $x \geqslant 0$ and $y \geqslant 0$) is analyzed.

The finite element analysis model $OCDEO$ is shown in Fig. 6b. Note that the dimensions of the model must be large enough to avoid any wave reflection from the boundaries CD and DE for the time duration considered here. By doing so, the model $OCDEO$ can be used to simulate the generalized thermoelastic response of the half space in Fig. 6a. The thermal loading is applied on OA, with its length being a. Lines AF and AG are accessory lines and will be used to discuss the results: the angle between AF and AE is $\pi/4$ and line AG is parallel to edge OC. It is worth emphasizing that the symmetry boundary conditions along OC must be enforced.

Fig. 7 shows the temperature contours at time $t = 0.05$ and 0.08, respectively. We can find that the temperature changed zone is restricted in a finite area and the temperature does not change out of this area. We can also find that the heat influence area gets larger with passage of time and there are zones with much greater gradient of the temperature than other area. That means the heat conducting at a finite speed. To exploit implication of these zones, temperature distribution along specific lines OC and AG in Fig. 7 is given by Figs. 8 and 9.

For $t = 0.08$ and 0.12, variation of the temperature along edge OC is plotted in Fig. 8. It is seen that the profile of the temperature versus distance curves resembles that for the one-dimensional problem (see Fig. 2): the temperature reduces abruptly to zero at the heat wave fronts (i.e., the second sound effect). This is corresponding to the large temperature gradient in Fig. 7. As mentioned earlier, although the second sound effect is also expected in two-dimensional problems in the generalized thermoelasticity, it is difficult to be captured in numerical simulations using the transform technology (Chen and Weng, 1988). However, the developed finite element method successfully predicts this delicate feature, showing its superiority over the transform method in the generalized thermoelasticity. Variation of the temperature along OC and AG at the instant $t = 0.08$ is given by Fig. 9. Again, there are jumps in the temperature distribution curves. It is

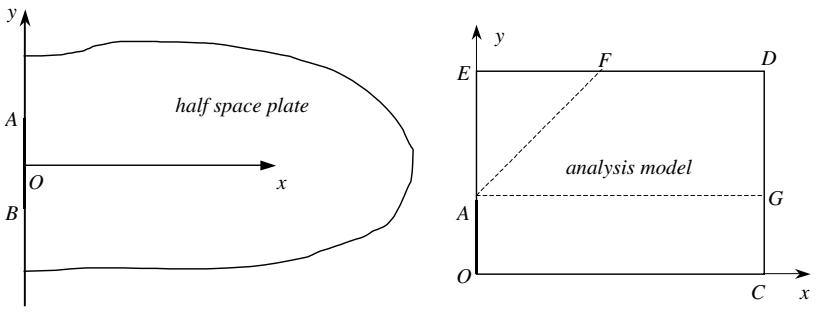

(a) Half space plate (b) Analysis model

Fig. 6. Half space subject to thermal shock loading.

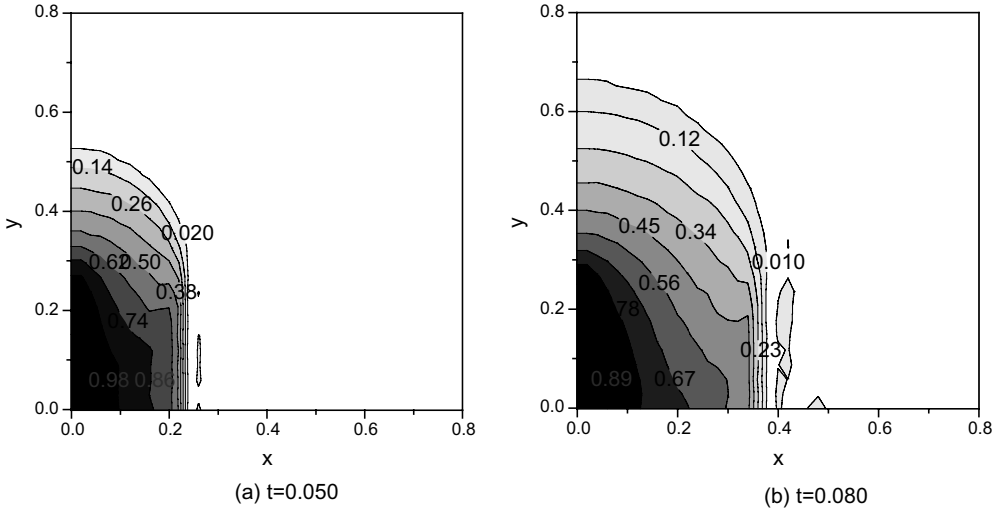

Fig. 7. The temperature of the plate at different time.

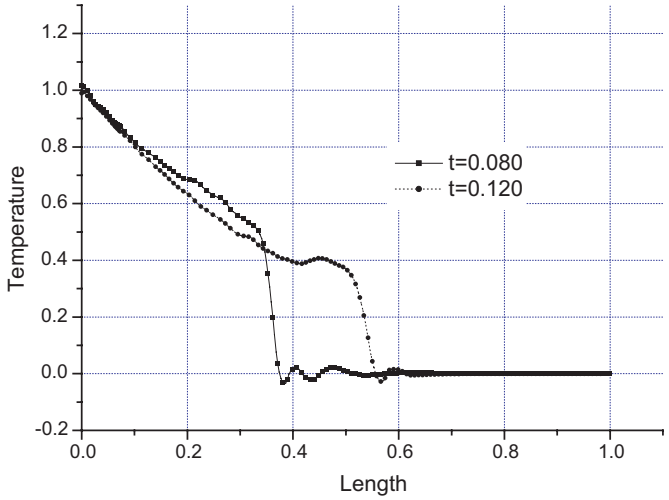

Fig. 8. The temperature distribution on edge OC at time $t = 0.08$ and 0.12.

also found that the temperature on OC is larger than on line AG. Noting that edge OC is adiabatic owing to the symmetrical condition whilst the heat close to line AG can conduct to the up direction. This causes the temperature along line AG smaller than that along OC.

Fig. 10 is the temperature on line OE at $t = 0.08$ and 0.12. The temperature about 1 in Fig. 10 is the temperature of segment OA where the heat source acted. Although the second sound effect of the heat conduction is obvious (the temperature of the plate does not change before the heat wave front arrives), the temperature varies continuously along AE without any jump. The reason is that the heat wave originated from different points along OA reaches the line AE at different time. As a result, the overall effect is that the points on AE are heated up continuously. The temperature distribution on line AF at time $t = 0.08$ and 0.12 is plotted in Fig. 11. The major features of the curves are shown to be the same as those given in Fig. 10.

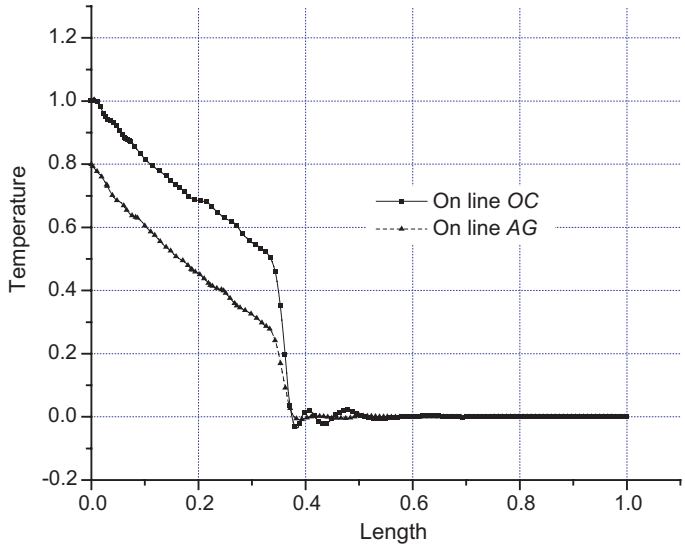

Fig. 9. The temperature on edge OC and line AG at time $t = 0.08$.

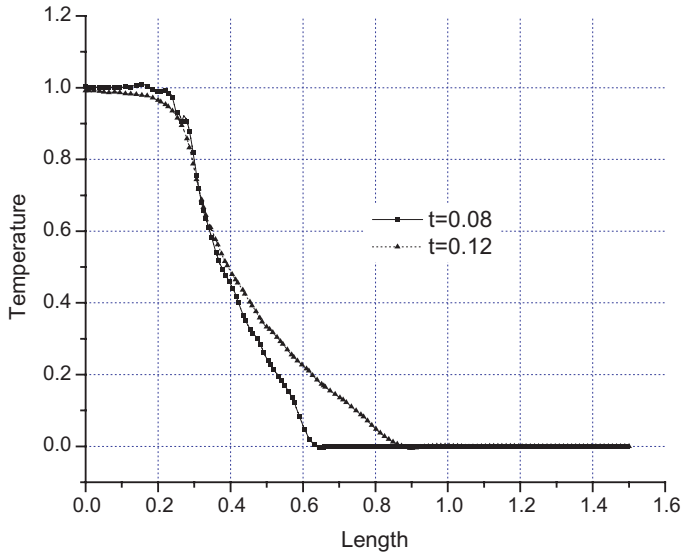

Fig. 10. The temperature distribution of edge AE at different time.

The property of displacement component u_x on edge OC is as the same as that in the slim strip (are shown in Figs. 4 and 5) and the displacement u_y on edge OC is zero due to the symmetrical boundary condition. The displacement components u_x and u_y on edge OE at different time are shown in Figs. 12 and 13, respectively. It is seen that the magnitude of the displacement on edge OE increases with time. It is apparent that the displacement is related to the heat conduction. It can be further inferred that the position at which the displacement vanishing corresponds to the heat wave front, in a support of previous findings that the heat wave traverses at finite speed.

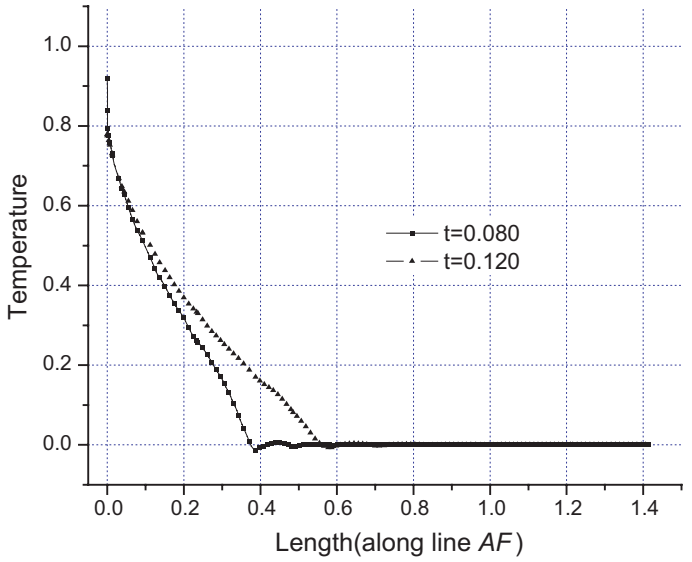

Fig. 11. The temperature on line AF at time $t = 0.08$ and 0.12.

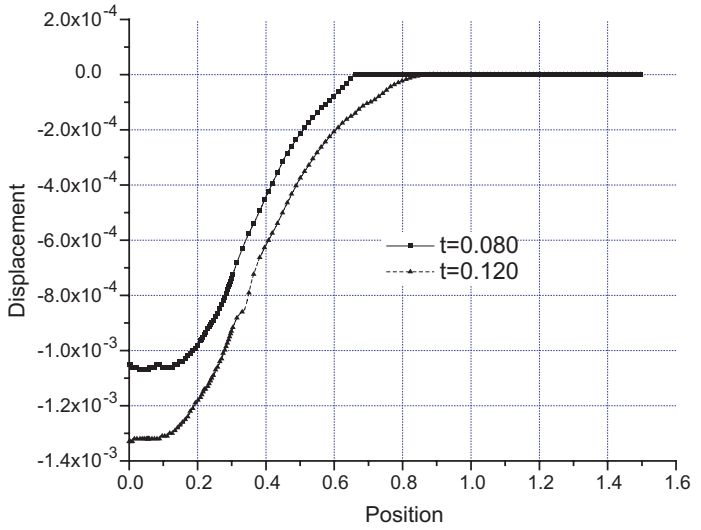

Fig. 12. The displacement u_x on edge OE at different time.

The stress σ_{xx} on edge OC at different time is shown in Fig. 14. Because the plate is traction free on the left side, the stress σ_{xx} of point 'O' is zero at any time. The shape of the stress is similar to the stress obtained in He et al. (2002) except the stress peak. According to the finite velocity conduction of heat, the heat wave front should be at $x = 0.268$, 0.590 and 0.805 at time $t = 0.060$, 0.132 and 0.180, respectively. We can find that the stress peak occurs at the heat wave front exactly and the magnitude of the stress peak reduces with time passing. The stress peak maybe associated with the large temperature gradient at the heat wave front and the magnitude reduces along with the temperature jump decreasing. We can forecast that the stress

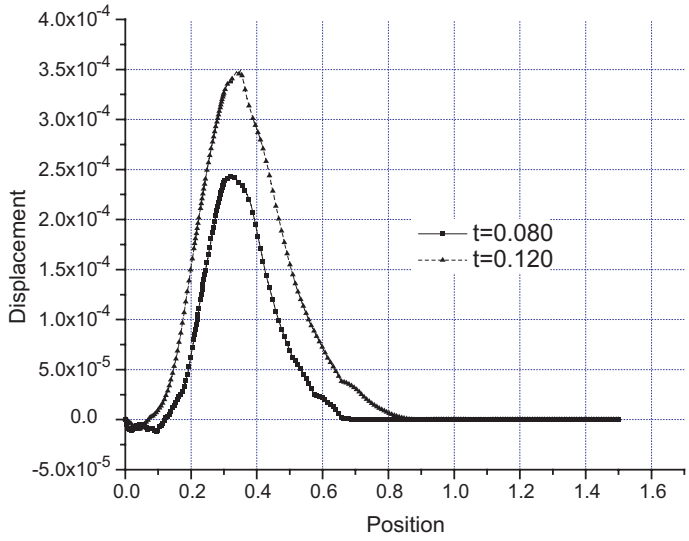

Fig. 13. The displacement u_y on OE at different time.

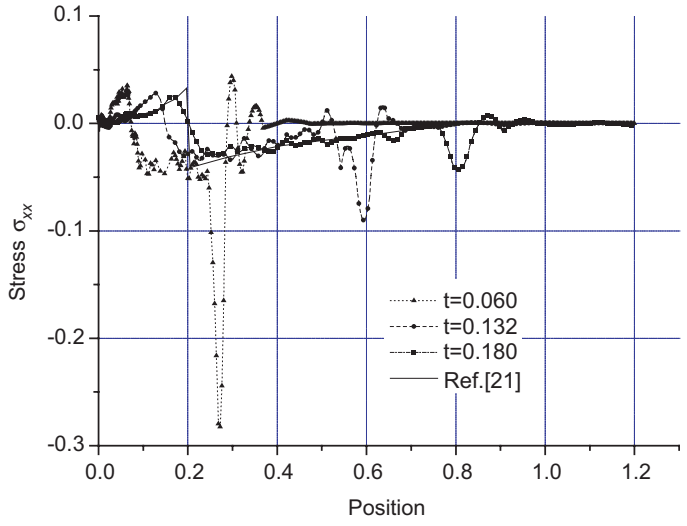

Fig. 14. The stress σ_{xx} on OC at different time.

peak will vanish when the temperature jump disappearing. The stress peak has not been observed in the *transform* method. We also find that the stress on the structure didn't change until the heat arrives.

5. Conclusions

The finite element equations corresponding to the generalized thermoelasticity with two relaxation time parameters are derived by sing the principle of virtual work. The equations are solved directly in time

domain with remeshing during the analysis. The numerical examples demonstrate that he developed method can faithfully predict the delicate second sound effect of heat conduction whilst this effect is usually difficult to be modeled by other methods (e.g., the transform method discussed in the Introduction section). The numerical results also show that there is a peak in the stress at the location of heat wave front and the magnitude of the peak reduces with time passing. It is expected that the developed finite element method can be applied to generalized piezothermoelastic and magnetothermoelastic problems.

Acknowledgments

This research was supported by the National Natural Science Foundation of China (10132010 and 10472089).

References

Anwar, M., Sherief, H., 1988. State space approach to generalized thermoelasticity. J. Therm. Stresses 11, 353–365.

Bonello, B., Perrin, B., Romatet, E., Jeannet, J.C., 1999. Application of the picosecond ultrasonic technique to the study of the elastic and time-resolved thermal properties of materials. Ultrasonics 35, 223–231.

Chen, J., Dargush, G.F., 1995. Boundary element method for dynamic poroelastic and thermoelastic analyses. Int. J. Solids Struct. 32 (15), 2257–2278.

Chen, T.C., Weng, C.I., 1988. Generalized coupled transient thermoelastic plane problems by Laplace transform/finite element method. J. Appl. Mech. 55, 377–382.

Chen, T., Weng, C., 1989. Coupled transient thermoelastic response in an axisymmetric circular cylinder by Laplace transform-finite element method. Comput. Struct. 33, 533–542.

Dhaliwal, R., Sherief, H., 1980. Generalized thermoelasticity for anisotropic media. Quart. Appl. Math. 33, 1–8.

Ei-caramany, A.S., Ezzat, M.A., 2004. Thermal shock problem in generalized thermo-viscoelasticity under four theories. Int. J. Eng. Sci. 42, 649–671.

Erbay, S., Suhubi, S., 1986. Longitudinal wave propagation in generalized thermoelastic cylinder. J. Therm. Stresses 9, 279–295.

Green, A.E., Lindsay, K.E., 1972. Thermoelasticity. J. Elasticity 2, 1–7.

He, T., Tian, X., Shen, Y.P., 2002. State space approach to one-dimensional thermalshock problem for a semi-infinite piezoelectric rod. Int. J. Eng. Sci. 40, 1081–1097.

He, T., Tian, X., Shen, Y., 2003. One-dimensional generalized thermal shock problem for a semi-infinite piezoelectric rod. Acta Mech. Sinica 35, 158–165.

Hostetler, J.L., Smith, A.N., Norris, P.M., 1998. Simultaneous measurement of thermophysical and mechanical properties of thin film. Int. J. Thermophys. 19, 569–577.

Ignaczak, J., 1979. Uniqueness in generalized thermoelasticity. J. Therm. Stresses 2, 171–175.

Lord, H., Shulman, Y., 1967. A generalized dynamical theory of thermoelasticity. J. Mech. Phys. Solids 15, 299–309.

Prevost, J.H., Tao, D., 1983. Finite element analysis of dynamic coupled thermoelasticity problems with relaxation times. J. Appl. Mech. 50, 817–822.

Sherief, H., 1993. State space approach to thermoelasticity with two relaxation times. Int. J. Eng. Sci. 31, 117–1189.

Sherief, H., 1994. A thermo-mechanical shock problem for thermoelasticity with two relaxation times. Int. J. Eng. Sci. 32, 313–325.

Sherief, H., Dhaliwal, R., 1980. A uniqueness theorem and variational principle for generalized thermoelasticity. J. Therm. Stresses 3, 223–230.

Sherief, H.H., Helmy, K.A., 2002. A two-dimensional problem for a half space in magneto-thermo-elasticity with thermal relaxation. Int. J. Eng. Sci. 40, 587–604.

Sherief, H.H., Megahed, F.A., 1999. A two-dimensional thermoelasticity problem for s half space subjected to heat sources. Int. J. Solids Struct. 36, 1369–1382.

Zhu, X., Vileneuve, D.M., Naumov, A.Y., Nikumb, S., Korkum, P.B., 1999. Experimental study of drilling sub-10 μm holes in thin metal foils with femtosecond laser pulses. Appl. Surf. Sci. 152, 138–148.